論文 / 著書情報
Article / Book Information

Title	Preparation and Characterization of Polyimide/Fluorinated Silicate Nano-hybrid Thin Films with Low Refractive Indices
Authors	Yulai HAN, Junji WAKITA, Shigeki KUROKI, Xiaogong WANG, Shinji ANDO
Citation	Journal of Photopolymer Science and Technology, Vol. 21, No. 1, p. 143-150
Pub. date	2008, 6

Journal of Photopolymer Science and Technology
Volume 21, Number 1 (2008) 143-150 © 2008CPST

Preparation and Characterization of Polyimide/Fluorinated Silicate Nano-hybrid Thin Films with Low Refractive Indices

Yulai HAN[1,2], Junji WAKITA[1], Shigeki KUROKI[1], Xiaogong WANG[2], and Shinji ANDO[1]*

[1]*Department of Chemistry & Materials Science*
Tokyo Institute of Technology, O-okayama, Meguro-ku, Tokyo, 152-8552, Japan
[2]*Institute of Polymer Science & Engineering,*
Department of Chemical Engineering, Tsinghua University, Beijing, 10084, China

A new series of polyimide (PI)-fluorinated silicate nano-hybrid materials with low refractive indices were prepared by the sol-gel process based on the PI derived from 4,4' (hexafluoroisopropylidene) diphthalic anhydride (6FDA) and 4,4'diaminodicyclohexyl-methane (DCHM). Triethoxy-1H,1H,2H,2H-tridecafluoro-*n*-octylsilane (13FTES) and tetraethoxysilane (TEOS) were employed to prepare the silicate precursors. Furthermore, 2-aminopropyl triethoxysilane (APrTEOS) was used as a coupling agent to improve the compatibility between the polymeric and inorganic domains of the nano-hybrid materials. The chemical structures of organo-silicate and hybrid materials were examined with solid state ^{29}Si- and ^{19}F-NMR and IR spectra. The thermal stability of PIs was not deteriolated with increasing the amount of TEOS, whereas it was sacrificed with the increase of 13FTES. The refractive indices of the hybrids can be controlled through the silica content, and low refractive indices were obtained for the prepared hybrid films. The PI/silicate nano-hybrid materials thus obtained are promising for high performance optical devices.

Key words: Polyimide; Fluorinated silicate; Hybrid material; Low refractive index; Thermal stability; Optical Transparency.

1. Introduction

Polyimides (PIs) are widely known to possess excellent properties and outstanding performance such as high thermal stability, good resistance to organic solvents, and thus they have been widely used in the fields of microelectronic devices, such as dielectric layers in multichip packaging and flexible printed circuits. Recently, lots of attentions have been paid to the optical properties of functional fluorinated PIs (FPI), in which the refractive index and optical transparency are key features in optical applications such as lens, optical waveguides, thin flexible waveplates and linear polarizers, and anti-reflective coatings [1].

PIs with low refractive indices have a wide range of potential applications in the fields of optical fibers, waveguides, and anti-reflective coatings. Groh et al.[2] have estimated the lowest limit of the refractive index of organic polymers using the empirical refractive increment methods. The numerical investigation revealed that very low refractive polymers could be obtained by exclusively using the following structural elements: $-CF_3$, $-OCF_2O$, $-CF_2$, $-C(CF_3)_2-$, $-CF(CF_3)_2$ and $-CH(CF_3)_3$. The authors and researchers in NTT corp. investigated the variations in the average refractive indices (n_{av}) of fluorinated polyimides (FPIs), and the results showed that the n_{av} of FPIs decreases linearly with increasing the fluorine content. [3–5]

Recently, lots of attention have been paid to the organic/inorganic nano-hybrid systems, in which both of the advantage of organic and inorganic components are expected to be integrated.[6] Moreover, they usually demonstrate novel properties that conventional materials do not possess, leading to materials with improved properties for electronic, optical, and photonic applications. Meanwhile, PIs have been considered as suitable polymer matrices for preparing advanced nano-hybrids that have potential applications in the fields of microelectronics and aircraft industries due to their excellent physical properties.[7] In the

Received April 8, 2008
Accepted May 23, 2008

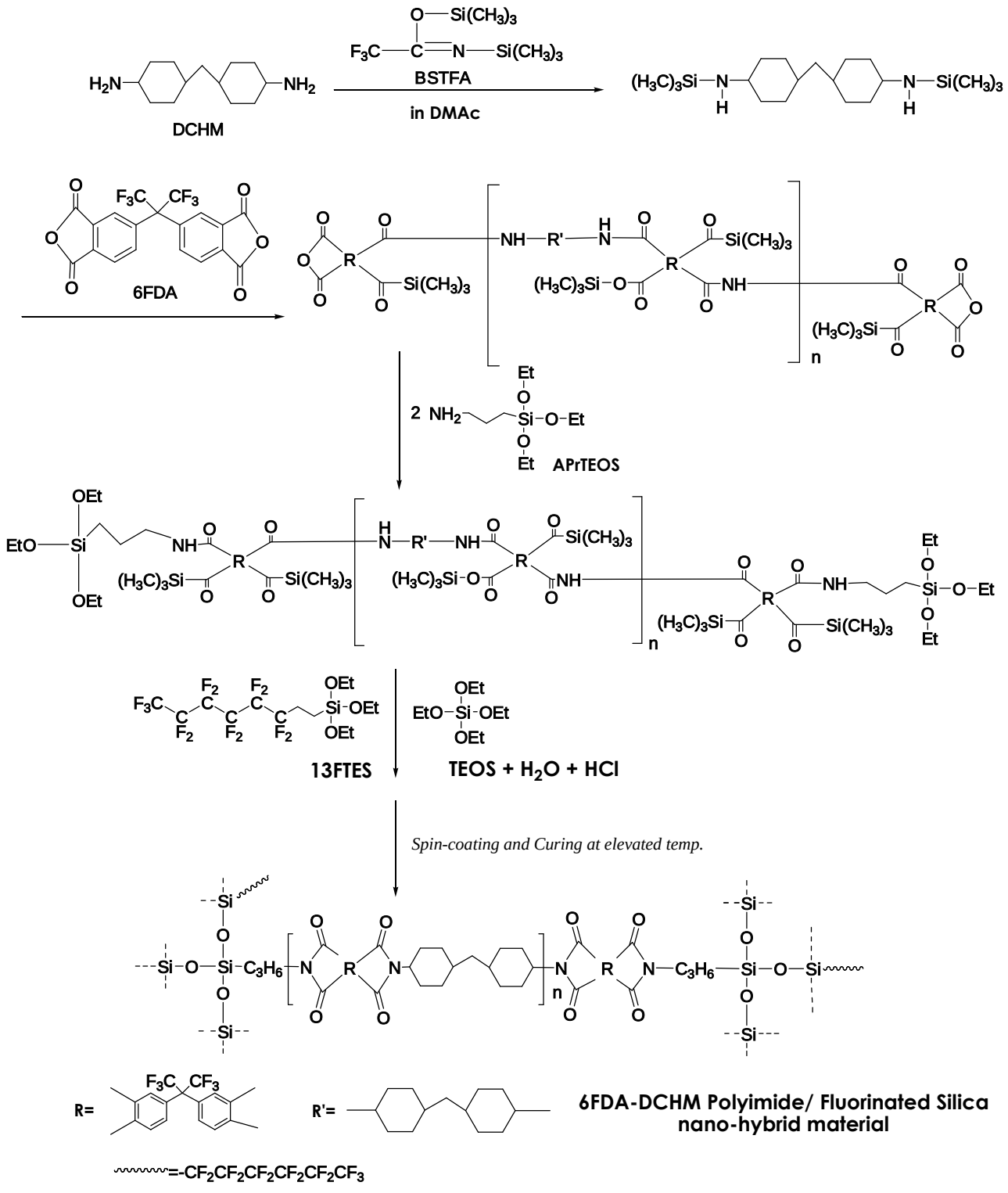

Fig.1 Reaction scheme for preparing fluorinated polyimide (PI)/fluorinated silicate nanohybrid materials.

nano-hybrid systems that have been reported, PI/silicate hybrid system has attracted particular interests.[8] However, most of the studies have been focusing on the mechanical and thermal properties, and only few studies have turned to such polymer/inorganic hybrid systems to decrease the refractive index of the resulting hybrid films, which is of vital importance for the optical and photonic applications.

In this study, a new series of PI/polymeric silicate nano-hybrids with low refractive indices were prepared by the sol-gel process with a fluorinated tetra-alkoxysilane and a coupling agent. Furthermore, the effects of coupling agent, the structure of inorganic domains in the hybrid materials, and the properties of the hybrids were discussed in detail.

2. Experimental

2.1. Materials

4,4'-(Hexafluoroisopropylidene) diphthalic dianhydride (6FDA) obtained from AZ Electronic Materials Co. Ltd. was purified by sublimation before use. 4-4'Diaminodicyclo-hexylmethane (DCHM) was first dissolved in *n*-hexane for recrystallization and then sublimated at 100ºC under reduced pressure for further purification. *N-N'*-Dimethylacetoamide (DMAc, anhydrous, 99.8%) purchased from Aldrich was dried with molecular sieve prior to use. *N,O*-Bis(trimethylsilyl) trifluoroacetamide (BSTFA,99+%) purchased from Aldrich was directly used as received. Tetra ethoxysilane (TEOS), triethoxy-1H,1H,2H,2H-tri decafluoro-*n*-octylsilane (13FTES) and 2-amino propyl triethoxysilane (APrTEOS) purchased from Tokyo Kasei were directly used as received.

2.2. Modified Silicate from TEOS and 13FTES

In this work, TEOS was used as a modifier of 13FTES to improve the compatibility with poly(amic acid)s and polyimides. Hence, we call hereafter the TEOS-modified 13FTES as "modified TEOS". To clarify the feasibility of the reaction between TEOS and 13FTES, fluorinated silicate gel was prepared from TEOS and 13FTES. The molar ratio between TEOS and 13FTES was kept as 3:1, and a 0.05N HCl solution was added to this system. The molar ratio of water and alkoxy groups was kept as 4:1. The solution was successively stirred at 60ºC for 4h and at 25ºC for 5h, and the resulting viscous solution was heated at 70ºC for 1 h, 150ºC for 1h and 220ºC for 1h to obtain a modified silicate.

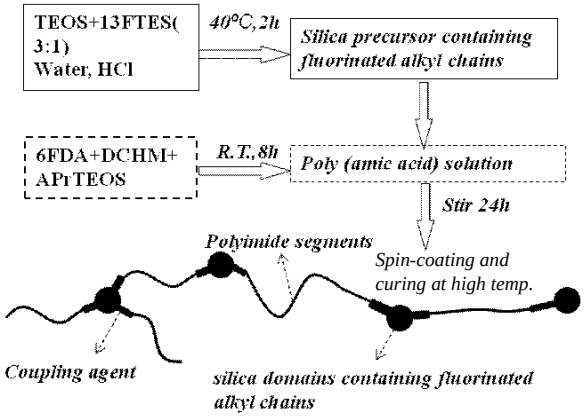

Fig.2 Scheme and procedure to prepare the precursor solution for PI/silica nanohybrid films and schematic structure of the main chains of the material.

2.3 Polyimide/Silicate Nanohybrid films

First, DCHM was added into a small glass bottle and dissolved in DMAc with stirring. After 5 min, BSTFA was slowly added into the solution and kept in ice bath. The molar ratio of BSTFA and DCHM was kept as 1.05 : 1. A paste-like solution was obtained after successive stirring for 30 min, and 6FDA was added into the solution and kept stirring for 3h. Then, APrTEOS were added by droplets into the solution. The molar ratio of 6FDA, DCHM and APrTEOS was kept as 5:4:2 to ensure the equal molar amounts of amino groups and anhydride groups in the main chain of poly(amic acid) (PAA). The solid concentration was fixed to 15 wt%. A transparent PAA solution was obtained after the solution was kept stirring for 5 h in ice bath.

Meanwhile, to obtain a silicate precursor solution, the mixture of TEOS, 13FTES and 0.05N HCl was kept stirring at 40ºC for 2h, and the solution was added into the above mentioned PAA solution and kept stirring for 24h to get a mixture of precursor solutions for PI/silicate hybrid films. Hybrid films were prepared through the spin-coating of solution onto Si substrates, dried at 70ºC for 1 h, and successive thermal imidization at 70ºC for 1 h, 150ºC for 1h and 220ºC for 1h under nitrogen flow. The chemical reactions for the preparation of hybrid films are shown in Figure 1 and a schematic diagram of the process is shown in Figure2.

2.4. Measurements

Infrared absorption spectra (IR) were obtained with an AVATAR-320 FT-IR spectrometer. Thermogravimetric analysis (TGA) was performed with

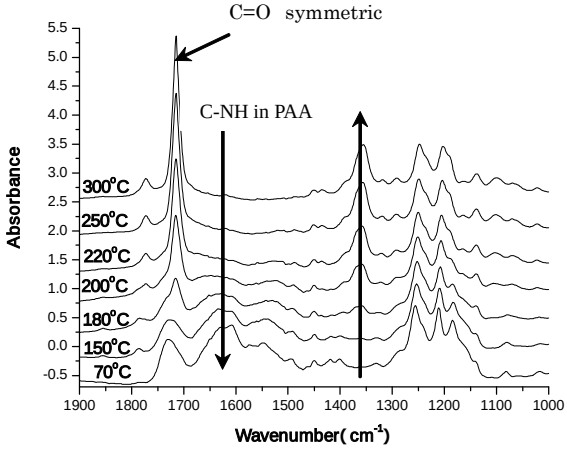

Fig.3 Variable temperature IR spectra of 6FDA/ DCHM PI films which follow imidization process.

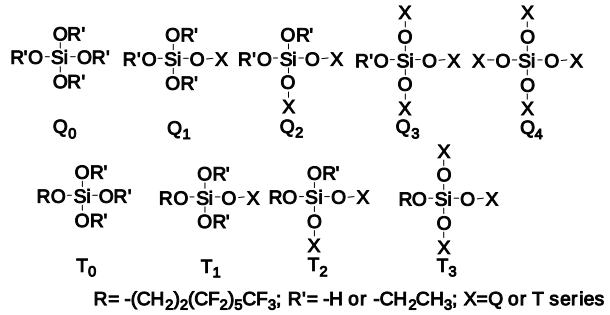

Fig.4 Possible fluorinated silicate structures formed by the sol-gel process.

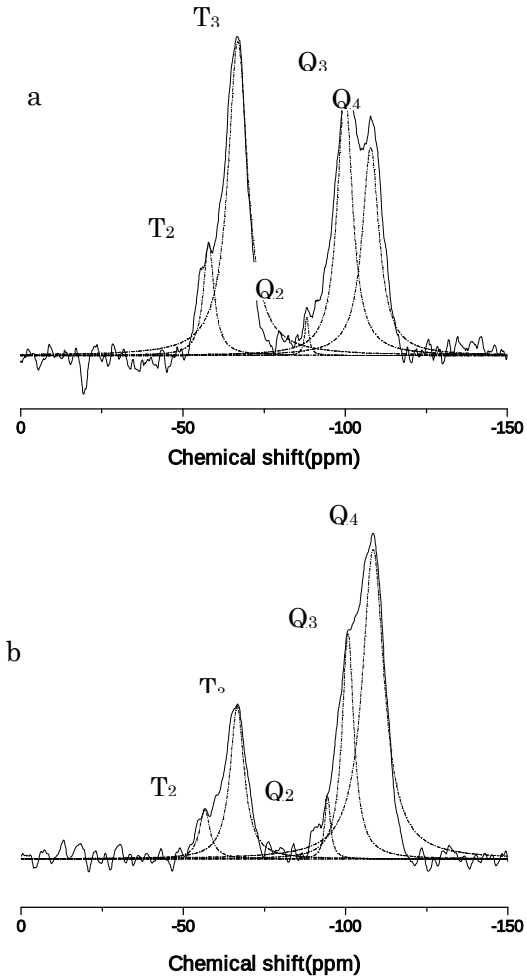

Fig.5 Solid state ^{29}Si spectra of the silicate derived from 13FTES-TEOS (a) CP/MAS spectrum with ^{1}H-enhanced intensities and (b) DD/MAS spectrum applicable to quantitative analysis.

a Shimadzu TGA-50 analyzer in the temperature range from room temp up to 900ºC at a heating rate of 10ºC/min under nitrogen. Visible-near infrared optical transmission spectra were acquired with Hitachi U-3500 spectrophotometer.

Direct polarization (DP) solid state ^{19}F MAS NMR experiments were performed with a JEOL EX-300 spectrometer operating at a resonance frequency of 282.7 Hz. The sample rotor was spun at a rate of 17 kHz, and $CFCl_3$ was used as a reference of ^{19}F chemical shifts (0 ppm). Solid state ^{29}Si cross polarization / magic angle spinning (CP/MAS) and dipolar decoupled / magic angle spinning (DD/MAS) NMR experiments were performed with a Bruker DSX-300 spectrometer operating at the resonance frequencies of 59.6 Hz for ^{29}Si. The sample rotor was spun at a rate of 16 kHz, and the contact time for polarization transfer was 2 msec. The repetition times for CP/MAS and DD/MAS were 5 sec and 10 sec, respectively. ^{29}Si chemical shifts were calibrated indirectly through the signal of poly(dimethyl siloxane) (–33.6 ppm from TMS).

The in-plane (n_{TE}) and out-of-plane (n_{TM}) refractive indices of PI films were measured with a prism coupler (Metricon, model PC-2010) equipped with half-waveplates in the light-path and He-Ne / semi-conductor laser sources. The in-plane / out-of-plane birefringence (Δn) was calculated as the difference between n_{TE} and n_{TM}. The average refractive index was calculated according to the equation: $n_{av} = [(2n_{TE}^2+n_{TM}^2)/3]^{1/2}$. All films were dried at 100ºC for 30 min under vacuum to remove the absorbed moisture.

3. Results and Discussion

3.1. Pristine 6FDA/DCHM PI films

Prior to the detailed study of nanohybrid films, pristine PAA and PI films of 6FDA-DCHM were characterized. Figure 3 shows the IR spectra of pristine PAA films cured at different temperatures, 70ºC, 150ºC, 180ºC, 200ºC, 250ºC and 300ºC respectively. The absorption peaks at 1727 cm^{-1} and 1620 cm^{-1} correspond to the C=O and C–NH

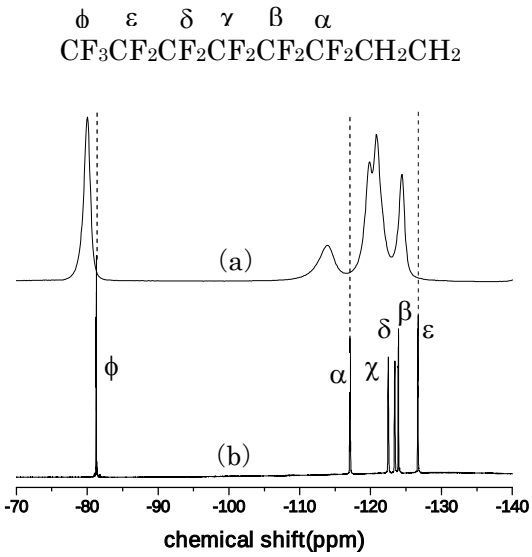

Fig.6 (a) Solid state ^{19}F MAS NMR of the silicate derived from 13FTES-TEOS and (b) liquid state ^{19}F NMR spectrum of 13FTES (neat).

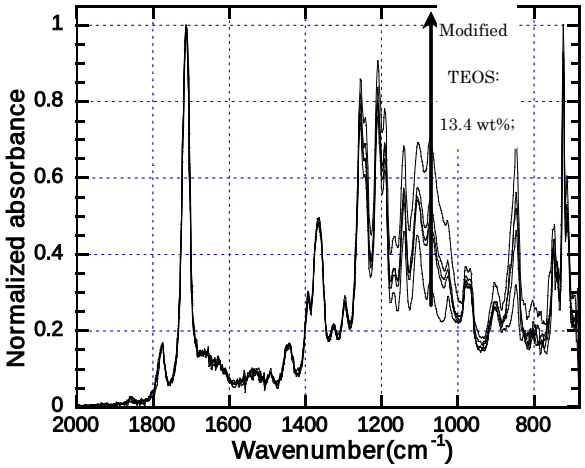

Fig.7 Normalized FT-IR spectra of PI/silicate nano-hybrid films with different amount of 13FTES.

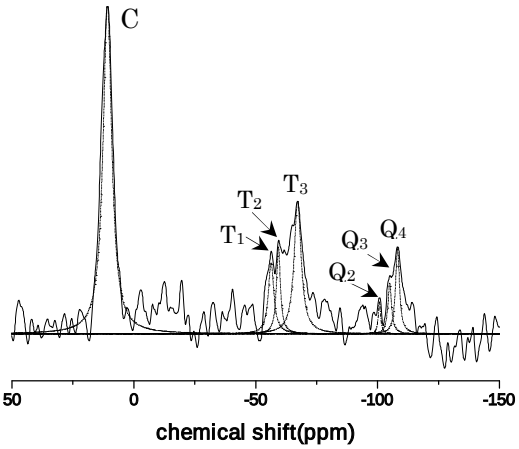

Fig.8 ^{29}Si DD/MAS NMR spectrum of PI/silicate nanohybrid films. The signal assignments are based on ref.13.

stretching in amic acid, respectively [8]. When the curing temperature arrived at 180ºC, three new peaks began to appear; peaks at 1774 cm^{-1}, 1712 cm^{-1} and 1354 cm^{-1}, which can be assigned to the asymmetric stretching of C=O, the symmetric C=O stretching, and the C-N stretching in PI, respectively, and those peaks become stronger with the increase of curing temperature. It should be noted that, when films were cured at 220ºC, the characteristic peak for PAA at 1620 cm^{-1} almost disappeared, which indicates that the thermal imidization was completed at around 220ºC.

3.2 Silicate derived from TEOS and 13FTES

The gelation behavior of the silicon alkoxide components and the formed structures of silicate components prepared from the multifunctional silicon alkoxide precursors were identified by solid state NMR spectra. First, the samples derived from the hydrolysis and polycondensation reactions of TEOS and 13FTES were characterized.

Here, a modified form of 'Q' notation was adopted to include the multifunctional system of this experiment [12]. The modifications for silicon-based tetrahedral containing oxygen and organic 'R' groups (R represents fluorinated alkyl chain in this experiment) are as follows: 'Q' represents quaternary oxygen tetrahedral, Q=Si($O_{1/2}$)$_4$; 'T' represents three oxygen group, one organic group terahedral, T= Si($O_{1/2}$)$_3$R. Figure 4 shows possible silicate structures formed through the sol-gel process in this experiment.

Figure 5 demonstrates the ^{29}Si CP/MAS and DD/MAS NMR spectra of samples derived from the mixture of 13FTES and TEOS. In spectrum (a), the sample exhibits five peaks at –108.0, –99.4, –89.0, –66.9 and –56.0 ppm which can be assigned to Q_4, Q_3, Q_2, T_3, and T_2 structures, respectively [13]. The ratio of the integrated intensities for Q and T structures obtained from DD/MAS spectrum is in agreement with the molar ratio of TEOS and 13FTES (Fig.5 (b)).

Figure 6 shows the solid state ^{19}F MAS NMR spectrum of the silicate derived from 13FTES and TEOS and the liquid state ^{19}F spectrum of neat 13FTES. The signals of 13FTES can be readily assigned to each of fluorine as follows: α: –117.17 ppm, β: –123.91 ppm, χ: –122.49 ppm, δ: –123.41 ppm, ε: –126.72 ppm according to the literature [14]. All the signals in the silicate spectrum are resonated at higher frequencies by 1.3~3.4 ppm

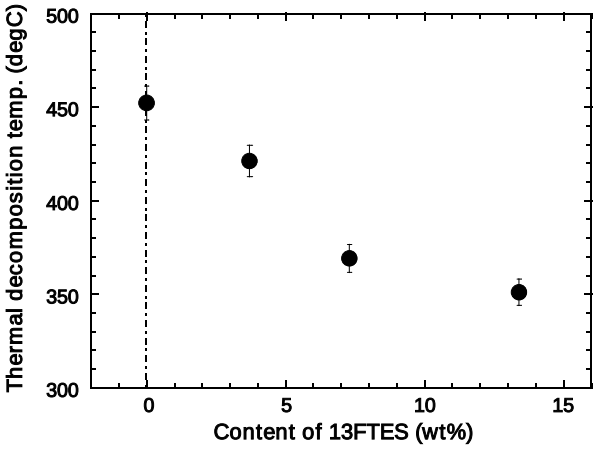

Fig.9 Variations in thermal decomposition temperature (T_d^5) of the nano-hybrid films prepared with different amounts of 13FTES.

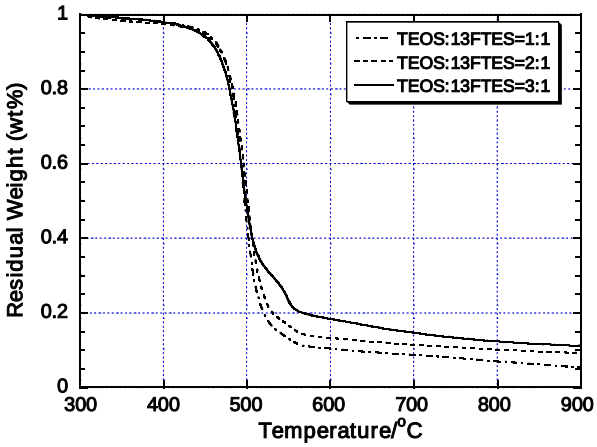

Fig.10 TGA thermograms of PI/silicate nano-hybrid films prepared with different amounts of TEOS.

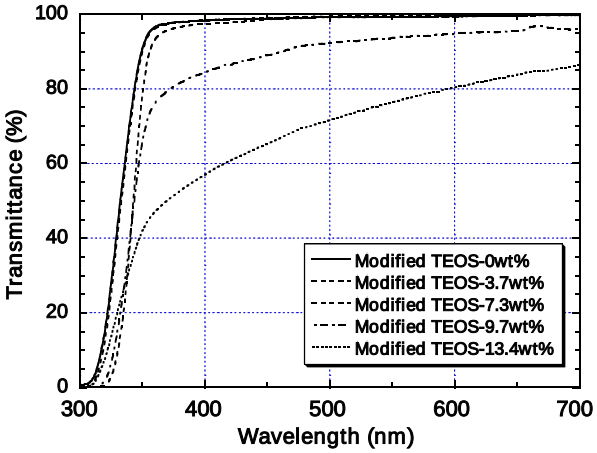

Fig.11 UV-vis transmission spectra of PI/silicate nano-hybrid films prepared with different amounts of modified TEOS (13FTES+TEOS).

than those of 13FTES, and no resonance from 13FTES and TEOS are observed. In addition, the peaks from β, δ and χ were merged together in the silicate spectrum, which suggests that fluorinated alkyl chains have been successfully introduced into the silicate samples. They are expected to be homogeneously distributed in the hybrid films.

3.3 PI / TEOS-13FTES Nano-hybrid Films

3.3.1 Structural Analysis

Figure 7 illustrates the normalized IR spectra of the prepared thin films with different amounts of modified TEOS. A broad Si–O–Si band with gradually increased intensity is observed around 1000~1100 cm^{-1}, which indicates the successful hydrolysis and polycondensation reactions of TEOS and 13FTES [15]. The peak around 1200 cm^{-1} corresponds to the C–F stretching, and its intensity also became stronger with the increasing amount of 13FTES, from which we could conclude that fluorinated alkyl chains have been introduced into the nano-hybrid thin films.

To further analyses of the exact structures of silicate domains and the function of coupling agent (APrTEOS), solid state ^{29}Si DD/MAS of PI/silicate nano-hybrids was measured. The resonant peaks in Figure 8 can be assigned as follows: Q_4: –108.3 ppm, Q_3: –104.8 ppm. Q_2: –100.8 ppm, T_3: –67 ppm, T_2: –59 ppm, T_1: –56 ppm. Another prominent peak C appearing at 10.4 ppm can be assigned to the Si atoms in APrTEOS as shown below [16]:

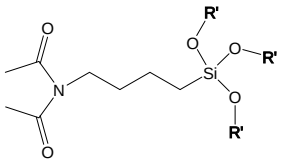

The structure mentioned above proves that APrTEOS indeed functions as a coupling agent, which can improve the compatibility between silicate and polymer chains in the system. It should also be noted that the molar ratio of APrTEOS and 13FTES is in agree with the integrated intensities of peak C and T series in the ^{29}Si DD/MAS NMR spectrum of nano-hybrid films, and the low percentage of Q series might be caused by the sublimation of TEOS.

3.3.2 Thermal Properties

Figure 9 shows the relationship between T_d^5 (5% weight-loss temperature under nitrogen flow) and the contents of 13FTES in the nano-hybrid films. It is obvious that the T_d^5 of the films decreases with increasing the amounts of 13FTES due to the thermally degradable ethyl and perfluoroalkyl moieties. The T_d^5 of the sample with 11 wt% of 13FTES is about 351ºC. A similar phenomenon was also observed by Nakagawa et al., in which

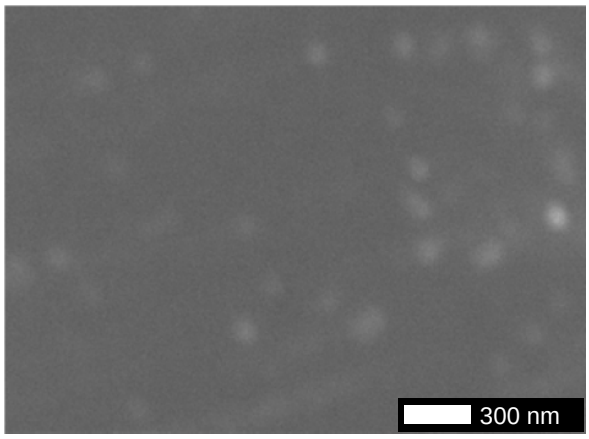

Fig.12 FE-SEM micrograph of PI/silica hybrid films (modified TEOS, 13.4 wt%, ×50,000). Silica particles larger than 50 nm cause light scattering.

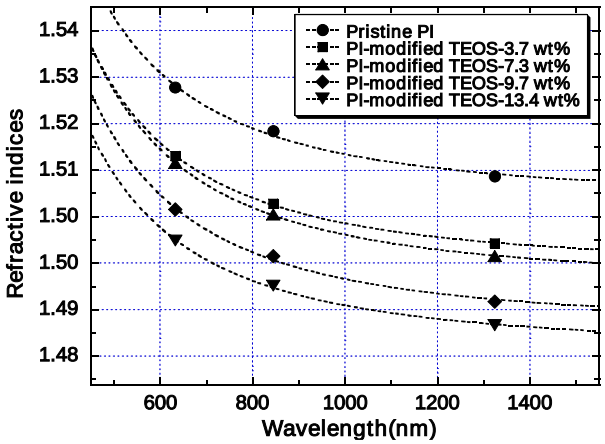

Fig.13 Refractive index dispersion of PI/Silica hybrid films in the visible and near-IR regions with different modified TEOS contents.

they employed $CF_3(CF_2)_7C_2H_4Si(OCH_3)_3$ as a source material to fabricate water repellent films. They reported the decomposition of C–F bond at around 400ºC. [17]

Figure 10 shows the thermal degradation behaviors of the PI/silicate nanohybrids with different amounts of modified TEOS (the contents of 13FTES were kept constant, 7 wt%). In contrast to the case with increasing 13FTES content, the TGA curves demonstrate that the thermal stability of the hybrid films was not deteriorated by increasing the amount of TEOS. In addition, the increase in residual weight above 700ºC suggests the successful incorporation of higher amounts of silica (SiO_2) into the nano-hybrid films that increases the ultimate thermal stability. This is also the advantage of the polymer/inorganic nano-hybrid materials.

3.3.3 Optical Properties

Figure 11 shows the UV-visible absorption spectra of hybrid films. The films are optically transparent when the contents of modified TEOS are less than 7.3 wt%. This can be attributed to the size of silicate particles which is significantly smaller than the wavelength of visible light so that scattering loss is minimized. In contrast, the hybrid films with modified TEOS higher than 7.3 wt% look opaque due to the larger silicate particles with increasing the precursor contents. As shown in the field emission (FE) SEM images (*see* Figure 12), the size of silicate particles is about 50~100 nm when the content of modified TEOS is 13.4 wt%. These particles may cause light scattering, which provides optically opaque films.

The refractive indices of the hybrid films are listed in Table 1 and Figure 13. The indices were measured at 632.8 nm, 845 nm and 1324 nm, and the plots in Fig.13 are fitted with the simplified Cauchy's formula; $n_\lambda = n_\infty + D/\lambda^2$, where λ is the wavelength, and D the dispersion coefficient. [18]

The refractive index was successfully decreased by about 1.7 % (n_{av}=1.4853 at 1324 nm) when the modified TEOS content is 13.4 wt%. It is well-known that refractive index (n_{av}) is closely related to density (ρ) and molecular polarizability (α) of materials as follows (Lorentz-Lorenz equation):

$$\frac{n_{av}^2+1}{n_{av}^2+2} = \frac{1}{3\varepsilon_0}\frac{\rho N_A}{M}\alpha = \frac{1}{3\varepsilon_0}K_p\frac{\alpha}{V_{vdw}}$$

, where N_A represents the Avogadro's number, M

Table 1. Thickness, in-plane (n_{TE}), out-of-plane (n_{TM}), and average (n_{av}) refractive indices, and birefringence (Δn) of PI/silicate hybrid films measured at 633, 845, and 1324 nm. The 0 wt% of 13FTES corresponds to the pristine PI.

13FTES content (wt%)	Thickness (μm)	λ=633 nm				λ=845 nm				λ=1324 nm			
		n_{TE}	n_{TM}	n_{av}	Δn	n_{TE}	n_{TM}	n_{av}	Δn	n_{TE}	n_{TM}	n_{av}	Δn
0	11.2	1.5281	1.5224	1.5262	0.0057	1.5207	1.5152	1.5187	0.0056	1.5124	1.5079	1.5109	0.0045
3	8.3	1.5157	1.5118	1.5144	0.0039	1.5076	1.5033	1.5062	0.0043	1.5007	1.4968	1.4994	0.0039
6	10.6	1.5144	1.5153	1.5132	0.0056	1.5059	1.5015	1.5044	0.0043	1.4985	1.4944	1.4972	0.0041
8	11.1	1.5067	1.5023	1.5052	0.0044	1.4986	1.4944	1.4972	0.0042	1.4908	1.4865	1.4894	0.0044
11	10.3	1.5008	1.4982	1.4999	0.0025	1.4935	1.4890	1.4921	0.0042	1.4868	1.4823	1.4853	0.0044

the molar mass of molecular, and V_{vdw} the van der Waals volume of the repeating unit. α/V stands for the polarizability per volume, which directly relates to the mobility of electrons. K_p stands for the packing coefficient, which reflects of the degree of molecular packing. The decrease in reflective indices in hybrid films can be attributed to a decrease of α/V by perfluoroalkyl moiety and to a low K_p owing to the formation of three dimensional Si–O–Si networks in the hybrid films. [19,20] In addition, it should be noted that the birefringence is also reduced by nano-hybridization with modified silicate, though the degrees of reduction are not proportional to the 13FTES contents. This should also be caused by the Si–O–Si networks which make the hybrid films more isotropic with lower degree of molecular orientation. The low birefringence is advantageous for waveguide and anti-reflective coating applications.

4. Conclusion

This study focused on the synthesis and characterization of a series of novel fluorinated PI/fluorinated silicate nano-hybrid films via the sol-gel reaction. The silicate structures and the function of APrTEOS as a coupling agent were characterized with FT-IR, solid state ^{29}Si and ^{19}F MAS NMR spectra. Silicate nano-particles with fluorinated alkyl chain has been successfully introduced into polyimide matrix by using a fluorinated tetra-alkoxysilane as a source material, and a series of low refractive thin films with high thermal stability, high transparency, and low birefringence were successfully obtained.

Acknowledgements

The authors acknowledge Mr. D. Yorifuji, Mr. Y. Takiue, Mr. S. Azami, Mr. A. Suzuki, and Mr. K. Takizawa at Tokyo Institute of Technology for the help of measurements of solid state ^{19}F NMR, variable-temperature FT-IR, refractive indices, TGA, and optical transparency.

References

1. G.O. Shonaike, S.G. Advani, *Advanced polymeric Materials*, CRC press, New York (2003).
2. W.Groh, A.Zimmerman, *Macromolecules*, **24**, 6660 (1991).
3. N.Koshoubu, T.Matsuura, T.Maruno, and S.Sasaki, *Polymer Prep. Jpn.*,**44** 316 (1995), *ibid*. **44**, 1521 (1995) *ibid*. **45,** 2305 (1996).
4. T. Matsuura, S. Ando, S. Sasaki, F. Yamamoto, *Macromolecules*, **24**, 5001 (1991), *ibid*. **25**, 3540 (1992), *ibid*. **26**, 419 (1993), *ibid*. **27**, 6665 (1994).
5. a) S. Ando, *J. Photopolym. Sci. Technol.*, **17**, 219 (2004). b) S. Ando, T. Matsuura, and S. Sasaki,'*Fluoropolymers 2: Properties*', Chap.14, G.Hougham, P. E. Cassidy, K. Johns, and T. Davidson, eds., Kluwer Academic/Plenum Pub., New York (1999).
6. G.Kickelbick, '*Hybrid Materials*', Wiley, Weinheim (2007) p.1.
7. Y.C.Ke, P.Stroeve, '*Polymer-layered Silicate and Silica Nanocomposites'*, Elsevier, New York (2005) p.198.
8. Ch.T. Yen, W.C. Chen, D.J. Liaw, *Polymer*, **44**, 7079 (2003).
9. P. Musto, G. Ragosta, G. Scarinzi, L. Mascia *Polymer*, **45**, 1697 (2004).
10. J.J. Lin, X-.D. Wang, *Polymer,* **48,** 318 (2007).
11. X.Y. Shang, Z.K. Zhu, J. Yin, and X.D. Ma, *Chem. Mater.* **14,** 71 (2002).
12. S.K. Young, W.L. Jarrett, K.A. Mauritz *polymer,* 43, 2311 (2002).
13. C.A. Fyfe, Y. Zhang and P. Aroca, *J. Am. Chem. Soc.*, **114**, 3252 (1992).
14. H.S. Zhang, T.E. Hogen-Esch, *Langumir,* **14,** 4972 (1998).
15. X.Y. Shang, Z.K. Zhu, J. Yin, X.D. Ma, *Chem. Mater.*, **14**, 71 (2002).
16. A. B. Scholten, J. W. de Haan, H. A. Claessens, L. J. M. von de Ven and C. A. Cramers, *J. Chromatogr. A*, **25**, 688 (1994).
17. H.J. Jeong , D.K. Kim, S.B. Lee, S.H. Kwon, K. Kadono, H.J. Jeong, *J. Colloid Interface Sci.* **13**, 235 (2001).
18. S. Ando, Y. Watanabe, and T. Matsuura, *Jpn. J. Appl. Phys., Part 1*, **41** 5254 (2002).
19. A. Matsumura, Y.Terui, S. Ando, A. Abe, and T. Takeichi, *J. Photopolym. Sci. Technol.*, **20**, 167 (2007).
20. Y. Terui and S. Ando, *High Perform. Polym.*, **18**, 825 (2006).